

Model Reference Adaptive Control for Hybrid Electric Vehicle With Dual Clutch Transmission Configurations

Walid Elzaghir¹, Yi Zhang, Narasimhamurthi Natarajan, Frank Massey, and Chunting Chris Mi², *Fellow, IEEE*

Abstract—This paper proposes the use of an adaptive control of a hybrid electric vehicle with dual clutch transmission (HDCT). First, this paper shows mathematical equations for the nonlinear system. Then it presents the linearized model for the proposed system. The control objective of the model reference adaptive controller (MRAC) considered in this paper is to minimize fuel consumption and reduce torque interruption in a hybrid electric vehicle. The MRAC can be used to control the electric motor during changes in speed and gear, and the system can adapt to a model that simulates different driver patterns. The effects of using different model responses as input combinations are analyzed in an effort to exploit the over-actuation feature of the system, as is the sensitivity of the performance to various design factors. The simulation results for an HDCT demonstrate that the MRAC achieves reduced torque interruption and less vehicle jerk compared to the conventional method of operation.

Index Terms—HEV, DCT, MRAC, control, simulation.

I. INTRODUCTION

HYBRID electric vehicles (HEV) with parallel architecture, and dual clutch transmission (DCT) are studied in this paper. These vehicles offer the flexibility of improving fuel economy and emissions without degrading safety and reliability parameters. The durability and performance enhancements of HEVs have encouraged the development of the appropriate power-train configurations and associated component resizing and control strategies.

The HDCT configuration consists of an internal combustion engine (ICE), an electric motor connected within the transmission, and a DCT, as shown in Fig. 1. To make full use of the HDCT power-train topology, frequent transitions between different modes are necessary to optimize the vehicle operation [1].

Manuscript received November 16, 2016; revised March 18, 2017 and August 6, 2017; accepted August 31, 2017. Date of publication September 12, 2017; date of current version February 12, 2018. The review of this paper was coordinated by Prof. T. M. Guerra. (*Corresponding author: Walid Elzaghir.*)

W. Elzaghir is with the Department of Information Systems Engineering, University of Michigan-Dearborn, Dearborn, MI 48128 USA (e-mail: walidelz@gmail.com).

Y. Zhang is with the Department of Mechanical Engineering, University of Michigan Dearborn, Dearborn, MI 48128 USA (e-mail: anding@umich.edu).

N. Natarajan is with the Department of Electrical and Computer Engineering, University of Michigan-Dearborn, Dearborn, MI 48128 USA (e-mail: natarasim@umich.edu).

F. Massey is with the Department of Mathematics and Statistics, University of Michigan-Dearborn, Dearborn, MI 48128 USA (e-mail: fmassey@umich.edu).

C. C. Mi is with the Department of Electrical and Computer Engineering, San Diego State University, San Diego, MI 92182 USA (e-mail: mi@ieee.org).

Color versions of one or more of the figures in this paper are available online at <http://ieeexplore.ieee.org>.

Digital Object Identifier 10.1109/TVT.2017.2751543

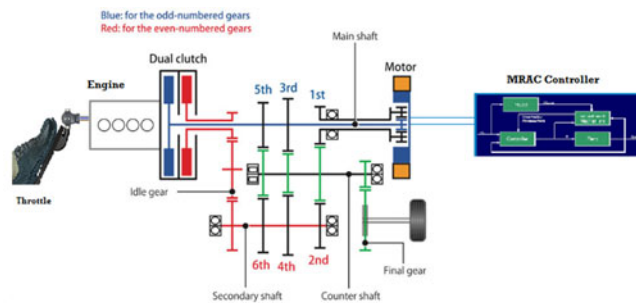


Fig. 1. The HDCT vehicle architecture

The torque produced by the ICE and the motor are combined at the transmission and the total torque is transferred to the wheels [2]. The DCTs have two input shafts. Therefore, by connecting an electric machine to one of the shafts, a hybrid dual clutch transmission can be obtained.

In an HDCT, the engine speed depends on the vehicle's speed. The power-train consists of only one electric machine, which can be made to operate both as a generator and as a motor, depending on the requirements thereby obtaining full hybrid functionality, in this case, the electric motor does not need to be high since the motor torque can be multiplied by the DCT, therefore, the power system consume less fuel. The first clutch is used for the odd gears and the second clutch is used for the even gears. The electric machine is connected to one of the input shafts and can use the 2nd, 4th, 6th and reverse gears, whereas the engine can use all the gears including the reverse gear.

This paper shows the feasibility of using model reference adaptive control (MRAC) to control the performance of the HDCT so that the driver can choose between different vehicle modes [3].

Two specific modes are addressed in this paper: (i) Sport Shifting Mode and (ii) Comfortable Mode.

- 1) Sport Shifting Mode: This mode allows the driver to feel the transmission shifting from one gear to another and have the manual transmission experience.
- 2) Comfortable Mode: This mode provides smooth transitions between gears.

The MRAC controller have been well established for many nonlinear problems, such as the Shunt active power-filter system [11], the Piezo-positioning system [13], the Three-phase three level boost rectifier [4], Controlling water level of boiler system [12], DC electric drive alone [8], and Control and Real-Time Optimization of Dry Dual Clutch Transmission during the Vehicle's Launch [14]. In addition, a model reference control law is proposed to coordinate the motor torque, engine torque,

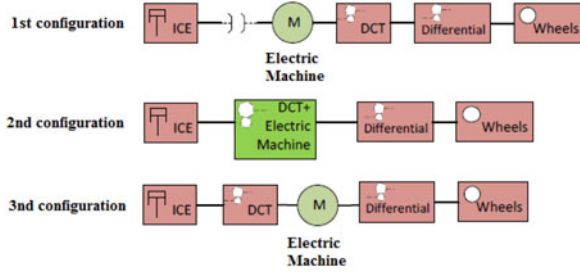


Fig. 2. Different parallel hybrid architecture.

and clutch torque to manage transitions to Series-Parallel Hybrid electric vehicle (SPHEVs) [15]. Although many researchers have studied dynamics and control during clutch engagement for conventional vehicles [16], [17], their strategies and conclusions are not directly applicable for the problem at hand, given the differences between HDCT and conventional vehicles. For HDCT, one more external torque, i.e., the motor torque, is applied to the powertrain, together with the engine torque. Others have applied the controller mechanism to SPHEV with conventional transmission only. Accordingly, their control objectives are different. For HDCT, the engine and the traction motor are two alternative power sources, and thus, the objective is to smoothly engage the clutch without causing torque interruption, regardless of which source is powering the vehicle.

A similar design has been patented by GM with two electric machines (one as generator), but was never developed as a product [5]. Our system is equipped with one motor that can serve as a generator as well, which makes the proposed design less expensive and the torque range of the EM does not need to be high since the EM torque can be multiplied by the DCT. Shown in Fig. 2 are some similar designs equipped with one motor only. The first configuration (EM connected before transmission) and the third configuration (EM connected after transmission) are similar to the power-train of the 'Audi A3-etrone' and 'P1-McLaren' respectively, exhibited at the March 2013 Geneva Motor Show. The second configuration (EM connected within transmission) is our design studied in the paper. The proposed design is different from the existing state of the art on controllers.

To the best of our knowledge, no relevant literature on MRAC with HDCT system (motor connected within transmission) problems have been found. This paper proposes a HDCT configuration with model reference adaptive control (MRAC) to cover the power lost by the engine during gear shifting or speed changes, with reduced drive-line interruption and frictional losses for HDCTs.

II. STATEMENT OF THE PROBLEM

The objective of this paper is to design a motor controller for HDCT topology so that the motor torque covers the torque lost by the engine during gear shifting or speed changes. In this respect, this design will minimize the fuel consumption, reduce torque interruption, and vehicle jerk due to shifting. The speed of the vehicle should track the desired performance of the adaptive control system specified by a reference model [6]. In this paper, a standard first-order response is chosen as the reference model [7]. The controller should be able to operate under the following three conditions:

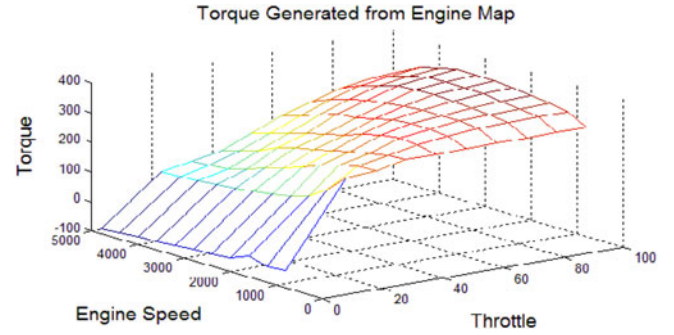


Fig. 3. Engine fuel map as a function of throttle and engine speed.

- 1) Vehicle operating under constant speed and the fuel injected into the ICE undergoes a step change. This is to study the ability of the motor controller to adapt to the torque output of the ICE.
- 2) Throttle is fixed but there is a step change in the desired speed. This is to study the ability of a motor controller to take over when the driver desires a rapid change in speed.
- 3) Throttle and speed are both fixed but the ICE gear changes. The motor controller should be able to mimic the typical behavior of a manual transmission (sport shifting mode) or mimic the typical behavior of an automatic transmission (comfortable mode).

III. THE EQUATIONS FOR THE DYNAMICS

The dynamic equations of each subsystem are provided in this section.

A. The Electric Motor

The equations for the electric motor [8] are

$$I_{mot} \frac{d\omega_{mot}}{dt} + b\omega_{mot} = Ki - T_{mot} \quad (1)$$

$$i = \frac{V_{dc} - \xi}{R}, \xi = K\omega_{mot}. \quad (2)$$

Eliminating i and ξ we get

$$I_{mot} \frac{d\omega_{mot}}{dt} + \left[b + \frac{K^2}{R} \right] \omega_{mot} = \frac{KV_{dc}}{R} - T_{mot} \quad (3)$$

where, I_{mot} is the effective inertia of the motor, i is the current in the armature circuit, T_{mot} is the torque delivered to the drive train by the motor, V_{dc} is the voltage supplied to the motor from the battery, b is the motor friction constant, K is the electromotive force constant, R is the resistance of armature circuit; and ω_{mot} is the motor speed in rad/s.

B. The Internal Combustion Engine

The characteristics of an internal combustion engine (ICE) can be represented by a nonlinear static map. The torque generated by the engine depends on the fuelling (u_{ic}) and the engine speed (ω_{ic}). The engine is modeled as a function of the current throttle input from the driver pedal (fuel) and the engine speed as shown in Fig. 3.

The engine torque can be expressed as,

$$T_{ic} = f(u_{ic}, \omega_{ic})$$

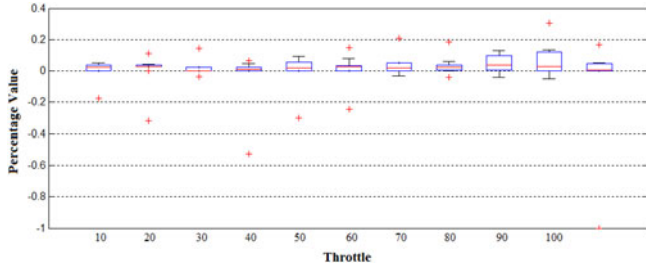


Fig. 4. Percentage change for fuel engine map and its approximation quadratic function.

where,

u_{ic} is the engine fuel input; ω_{ic} is the engine speed in rad/s.

We approximate $f(u_{ic}, \omega_{ic})$ by a quadratic function in u_{ic} and ω_{ic} , the resulting engine torque equation can be written as,

$$T_{ic} = (c_{11}\omega_{ic}^2 + c_{12}\omega_{ic} + c_{13})u_{ic}^2 + (c_{21}\omega_{ic}^2 + c_{22}\omega_{ic} + c_{23})u_{ic} + (c_{31}\omega_{ic}^2 + c_{32}\omega_{ic} + c_{33}). \quad (4)$$

C_{ij} (for $i, j = 1, 2, 3$) are constant values derived for the approximation of the quadratic function of the fuel map using the Maxima tool. Fig. 4 quantify the percentage change for fuel engine map and its approximation from quadratic function.

Applying Newton's 2^{nd} law, we obtain,

$$I_{ic} \frac{d\omega_{ic}}{dt} = T_i - T_{ic} \quad (5)$$

where,

I_{ic} is the effective inertia of engine, T_i is the torque generated by the ICE, and T_{ic} is the torque delivered to the drive train.

C. Dual Clutch Transmission

A DCT combines the convenience of an automatic transmission with the fuel efficiency of a manual transmission. It houses two separate clutches, one for odd and one for even gear sets, eliminating the need for a torque converter. To ensure smooth shifting and optimal efficiency, DCTs need sophisticated controllers capable of preselecting the next gear and engaging the appropriate clutch precisely when required.

The torque transmitted through DCT can be expressed as,

$$I_{DCT} \frac{d\omega_{DCT}}{dt} = T_i - T_{DCT}$$

where T_{DCT} is the torque carried by DCT, ω_{DCT} and I_{DCT} are the speed and the mass moments of inertia of the flywheel, respectively.

For the sake of easily designing the controller, further assumptions about motional relationship among the output shafts of transmission and the engine speed should meet the equations $\omega_{ic} = \omega_{DCT}$, $\omega_{mot} = \omega_{ic} (i_{mot}/i_{ic})$ and the gear imposes a single constraint, specified by the fixed gear ratio, consequently the DCT equation is embedded into the HDCT plant equation. Then the HDCT simplified model is shown in Fig. 5.

The power split ratio u for HDCT design is defined as the power request to the motor (P_{mot}) divided by the total power

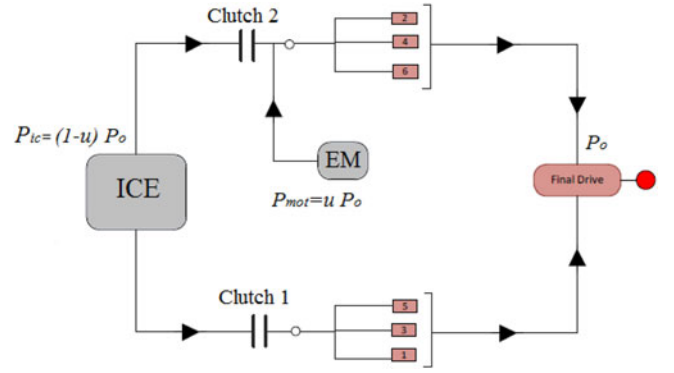


Fig. 5. Schematic of hybrid dual clutch transmission.

request at the wheels (P_o), which can be expressed as,

$$u = \frac{P_{mot}}{P_o}.$$

Therefore, ICE torque and power are given by,

$$T_{ic} = \frac{(1-u)}{i_{ic}} T_o, \quad P_{ic} = (1-u)P_o.$$

Motor torque and power are given by,

$$T_{mot} = \frac{(u)}{i_{mot}} T_o, \quad P_{mot} = uP_o.$$

D. The Hybrid System of the Motor, Engine and DCT

Both the engine and the motor provide the required power to the drive shaft, depending on the vehicle speed. The vehicle torque output can be expressed as,

$$T_o = i_{mot} T_{mot} + i_{ic} T_{ic}. \quad (6)$$

where, i_{mot} and i_{ic} are a constant ratio.

The longitudinal vehicle dynamics can be expressed as,

$$F_p = mg(f_0 + f_1 v) + mg \sin \theta + \frac{1}{2} \rho C_D A v^2 \quad (7)$$

where, C_D is the aerodynamic drag coefficient, v is the vehicle speed, f_0 and f_1 are the friction force constants, and $mg \sin \theta$ is the incline force.

Applying Newton's law yields,

$$m \frac{dv}{dt} = \frac{T_o}{r} - F_p \quad (8)$$

and the hybrid plant equation is,

$$\frac{dv}{dt} = C_0 + C_1 v + C_2 v^2 + B V_{dc} \quad (9)$$

where, C_0 , C_1 , C_2 and B can be expressed as shown at the bottom of the next page.

Following assumptions are made for (9):

- 1) The slope of the road is assumed to be negligible.
- 2) When the throttle is constant: C_0 , C_1 , C_2 and B are always constant parameters.
- 3) When the throttle is varying, the parameters will vary slowly and the switching from one value to another occurs at low frequencies. In the throttle change case, there should be enough time between changes so that θ_t^* can

guarantee closed loop stability and the adaptive law has time to “learn” about the change in the parameters, the same approach as above can be used to show that the error will be bounded, provided the switching frequency is sufficiently small, as shown in Fig. 7.

The system described by (9) can be easily converted to a first order linear system using feedback linearization. We are primarily interested in systems where v tracks a desired speed profile v_d , and it is slightly more intuitive to write the control law as,

$$V_{dc} = \theta_1 v_d + \theta_2 (v_d - v) + \theta_3 + \theta_4 v^2. \quad (10)$$

Note that the feedback law given in (10) can be written in a concise form as,

$$\mathbf{V}_{dc} = [\theta_1 \quad \theta_2 \quad \theta_3 \quad \theta_4] \begin{bmatrix} v_d \\ v_d - v \\ 1 \\ v^2 \end{bmatrix} = \theta \Phi \quad (11)$$

The choice of the symbols θ and Φ is to be consistent with the generally accepted notation used in MRAC, and θ is a vector of gains to be determined. The gains θ_i can be expressed as,

$$\theta_1 = \frac{(-C_1 - a_m + b_m)}{B}; \theta_2 = \frac{(C_1 + a_m)}{B}$$

$$\theta_3 = \frac{-C_0}{B}; \theta_4 = \frac{-C_2}{B}.$$

The above choice of gains will result in the following closed loop system,

$$\frac{dv}{dt} = -a_m v + b_m v_d.$$

This shows that by proper choice of the gains, we can obtain any first order linear system behavior.

In the next section, we briefly introduce the key results concerning the model reference adaptive control (MRAC) to show how we can design an adaptive control so that the gains can be tuned in real time to achieve any first order linear system behavior.

IV. THE ADAPTIVE CONTROL LAW

A. The MRAC Architecture

The MRAC architecture (as shown in Fig. 6) contains a reference model that is built to match the desired powertrain

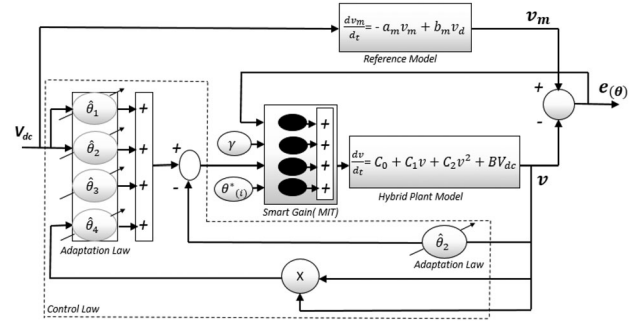


Fig. 6. The MRAC architecture for HDCT.

dynamics of the driving mode. An output feedback MRAC algorithm will be proposed, the conditions for closed-loop system stability will be derived, and the methods for selecting input combinations and controller parameters will be discussed. The discussions and experimental results presented will establish the effectiveness of the proposed MRAC.

B. The MIT Rule

The gradient method, also referred as the MIT rule, was developed by the Instrumentation Laboratory at the Massachusetts Institute of Technology (MIT) [9]. It will be assumed that in the closed loop system, the controller has one adjustable parameter θ . The parameter $e(\theta)$ represents the error between the output of the plant ($y_{plant}(\theta)$) and the output of the model reference ($y_{model}(\theta)$). The goal here is to adjust θ to minimize the cost function $J(\theta) = \frac{1}{2} e^2(\theta)$ [10].

- 1) The tracking error is: $e(\theta) = y_{plant}(\theta) - y_{model}(\theta)$
- 2) The form cost function is: $J(\theta) = \frac{1}{2} e^2(\theta)$
- 3) The update rule is: $\frac{d\theta}{dt} = -\gamma \frac{\delta J}{\delta \theta} = -\gamma e \frac{\delta e}{\delta \theta}$

It is important to highlight that change in θ is proportional to the negative gradient of $J(\theta)$.

C. The Adaptive Control Law

The adaptive control law is very general. Here, we focus on a special case of a first order system where the model is a stable linear system. The adaptation is a set of feedback gains, and the control signal given in (11) for the MIT rule can be expressed as,

$$\dot{\theta} = -\gamma \Phi^T e. \quad (12)$$

$$C_0 = \frac{r(c_{13} i_{ic} u_{ic}^2 + c_{23} i_{ic} u_{ic} - mg r \sin \theta - f_0 mg r + c_{33} i_{ic})}{I_T},$$

$$C_1 = -\frac{i_{mot} I_T B K - c_{12} i_{ic}^2 r u_{ic}^2 - c_{22} i_{ic}^2 r u_{ic} + f_1 mg r^3 + b i_{mot}^2 r - c_{32} i_{ic}^2 r}{I_T r},$$

$$C_2 = -\frac{\frac{1}{2} \rho C_D r^3 A - c_{11} i_{ic}^3 u_{ic}^2 - c_{21} i_{ic}^3 u_{ic} - c_{31} i_{ic}^3}{I_T r},$$

$$B = \frac{i_{mot} r K}{I_T R},$$

$$I_T = m r^2 + i_{mot}^2 I_{mot} + i_{ic}^2 I_{ic}.$$

In terms of each gain, the above formula is decoupled and can be written as,

$$\dot{\theta}_1 = -\gamma v_d e; \dot{\theta}_2 = -\gamma (v_d - v) e; \dot{\theta}_3 = -\gamma 1 e; \dot{\theta}_4 = -\gamma v^2 e.$$

V. PROVING THE CONTROL LAW AND STABILITY USING LYAPUNOV'S METHOD

The adaptive control of non-linear plants using the MRAC method is discussed next. The hybrid system developed from the complex system can be represented using the following first-order differential equation,

$$\frac{dv}{dt} = C_0 + C_1 v + C_2 v^2 + B V_{dc}. \quad (13)$$

where, v and V_{dc} represent plant output and input, respectively, and v^2 denotes the quadratic engine map.

A. Problem Specification

Let the desired performance of the adaptive control system be specified by a first-order reference model,

$$\frac{dv_m}{dt} = -a_m v_m + b_m v_d. \quad (14)$$

where, a_m and b_m are constant parameters and v_d is a bounded external reference signal. The parameter a_m is required to be strictly positive to ensure stability of the reference model, and b_m is chosen to be strictly positive without loss of generality [10]. The motivation behind using the adaptive control design is to formulate a control law and an adaptation law such that the resulting error $v - v_m$ asymptotically converges to zero.

B. Choice of Control Law

As the first step in the adaptive controller design, let us choose the control law to be,

$$V_{dc} = \hat{\theta}_1 v_d + \hat{\theta}_2 (v_d - v) + \hat{\theta}_3 + \hat{\theta}_4 v^2. \quad (15)$$

where, $\hat{\theta}_1$, $\hat{\theta}_2$, $\hat{\theta}_3$, and $\hat{\theta}_4$ are variable feedback gains. With this control law, the closed-loop dynamics can be expressed as,

$$\begin{aligned} \frac{dv}{dt} &= (C_1 - B\hat{\theta}_2)v + (B\hat{\theta}_1 + B\hat{\theta}_2)v_d + B\hat{\theta}_3 \\ &+ C_0 + (B\hat{\theta}_4 + C_2)v^2. \end{aligned} \quad (16)$$

If the plant parameters were known, the values of the control parameters would be (initial values),

$$\begin{aligned} \theta_1^* &= \frac{(-C_1 - a_m + b_m)}{B}; \theta_2^* = \frac{(C_1 + a_m)}{B} \\ \theta_3^* &= \frac{-C_0}{B}; \theta_4^* = \frac{-C_2}{B} \end{aligned}$$

which would lead to closed-loop dynamics identical to the reference model dynamics, and yield zero tracking error. In this case, the first term in (15) would result in the right DC gain, while the second term in the control law (15) would achieve the dual objectives of canceling the term $C_1 v$ in (13) and imposing the desired pole $a_m v_m$.

In the adaptive control problem, since C_0 , C_1 , C_2 and B are unknown, the control input will achieve these objectives adaptively, i.e., the adaptation law will continuously search for

the right gains, based on the tracking error $v - v_m$, so as to make v tend to v_m asymptotically.

C. Choice of Adaptation Law

The adaptation law for the parameters $\hat{\theta}_1$, $\hat{\theta}_2$, $\hat{\theta}_3$ and $\hat{\theta}_4$ can be chosen as follows.

Let,

$$e = v - v_m, \quad (17)$$

be the tracking error. The error of each parameter is defined as the difference between the controller parameter provided by the adaptation law and its corresponding ideal parameter, i.e.,

$$\tilde{\theta}(t) = \begin{bmatrix} \tilde{\theta}_1 \\ \tilde{\theta}_2 \\ \tilde{\theta}_3 \\ \tilde{\theta}_4 \end{bmatrix} = \begin{bmatrix} \hat{\theta}_1 - \theta_1^* \\ \hat{\theta}_2 - \theta_2^* \\ \hat{\theta}_3 - \theta_3^* \\ \hat{\theta}_4 - \theta_4^* \end{bmatrix} \quad (18)$$

The dynamics of the tracking error can be found by subtracting (16) from (14) results in,

$$\begin{aligned} \frac{de}{dt} &= \frac{dv}{dt} - \frac{dv_m}{dt} \\ \frac{de}{dt} &= (C_1 - B\hat{\theta}_2)v + (B\hat{\theta}_1 + B\hat{\theta}_2)v_d + B\hat{\theta}_3 + C_0 \\ &+ (B\hat{\theta}_4 + C_2)v^2 + a_m v_m - b_m v_d. \end{aligned} \quad (19)$$

Thus, the adaptation law can be expressed as,

$$\dot{\hat{\theta}}_1 = -\gamma e v; \dot{\hat{\theta}}_2 = -\gamma e v_d; \dot{\hat{\theta}}_3 = -\gamma e; \dot{\hat{\theta}}_4 = -\gamma e v^2.$$

D. Tracking Convergence Analysis

With the control law and adaptation law chosen above, we can now analyze the system's stability and convergence behavior using Lyapunov theory. The Lyapunov candidate function can be expressed as,

$$\begin{aligned} V &= \frac{1}{2}e^2 + \frac{B}{2\gamma}(\hat{\theta}_1 - \theta_1^*)^2 + \frac{B}{2\gamma}(\hat{\theta}_2 - \theta_2^*)^2 \\ &+ \frac{B}{2\gamma}(\hat{\theta}_3 - \theta_3^*)^2 + \frac{B}{2\gamma}(\hat{\theta}_4 - \theta_4^*)^2. \end{aligned} \quad (20)$$

It is important to note that the error goes to zero if the parameters of the controller are set to the initial values. This function is zero only when the error is zero and the controller parameters have the correct values. The derivative of V is given as,

$$\begin{aligned} \frac{dV}{dt} &= \frac{de}{dt}e + \frac{B}{\gamma}(\hat{\theta}_1 - \theta_1^*)\dot{\hat{\theta}}_1 + \frac{B}{\gamma}(\hat{\theta}_2 - \theta_2^*)\dot{\hat{\theta}}_2 \\ &+ \frac{B}{\gamma}(\hat{\theta}_3 - \theta_3^*)\dot{\hat{\theta}}_3 + \frac{B}{\gamma}(\hat{\theta}_4 - \theta_4^*)\dot{\hat{\theta}}_4. \end{aligned} \quad (21)$$

Substituting (19) into (21) with the values

$$a_m = -C_1 + B\theta_2^*; b_m = B(\theta_1^* + \theta_2^*)\Delta\theta_x = \hat{\theta}_x - \theta_x^*$$

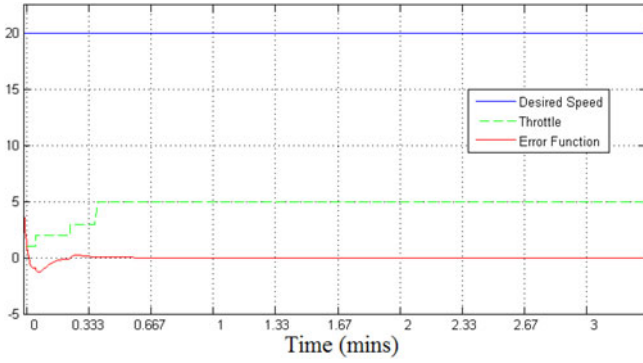


Fig. 7. Error function converges to Zero.

yields

$$\begin{aligned} \frac{dV}{dt} = & e[C_1 v - B\hat{\theta}_2 v + B\hat{\theta}_1 v_d + B\hat{\theta}_2 v_d + B\hat{\theta}_3 \\ & + (B\hat{\theta}_4)v^2 + a_m v_m - B\theta_1^* v_d - B\theta_2^* v_d] \\ & + \frac{B}{\gamma}(\Delta\theta_1)(-\gamma e v) + \frac{B}{\gamma}(\Delta\theta_2)(-\gamma e v_d) \\ & + \frac{B}{\gamma}(\Delta\theta_3)(-\gamma e) + \frac{B}{\gamma}(\Delta\theta_4)(-\gamma e v^2). \end{aligned} \quad (22)$$

If the parameters are updated as

$$\dot{\hat{\theta}}_1 = -\gamma e v; \dot{\hat{\theta}}_2 = -\gamma e v_d; \dot{\hat{\theta}}_3 = -\gamma e; \dot{\hat{\theta}}_4 = -\gamma e v^2 \quad (23)$$

The resulting derivative of the Lyapunov candidate function can be expressed as,

$$\frac{dV}{dt} = -a_m(v - v_m)e. \quad (24)$$

and

$$e = v - v_m$$

and therefore the final result is given as,

$$\frac{dV}{dt} = -a_m e^2.$$

Thus, the adaptive control system is globally stable, i.e., the signals e , $\hat{\theta}_1$, $\hat{\theta}_2$, $\hat{\theta}_3$ and $\hat{\theta}_4$ are bounded. Furthermore, the tracking error ($e(t)$) is guaranteed to be asymptotically convergent to zero because the boundedness of e , θ_1^* , θ_2^* , θ_3^* and θ_4^* implies the boundedness of $e(t)$, which implies the uniform continuity of V .

As a result, the error function will converge to zero, for the adaptive control system is globally stable. A short analysis of Fig. 7 reveals the powerful development of the control system and demonstrates its adjustability.

VI. RESULTS AND DISCUSSION

To demonstrate the effectiveness of the MRAC control under both tracking and regulatory conditions, the performance of the engine and DC motor is simulated under various operating conditions, such as varying the speed, varying the throttle, and shifting the gears, for both the DCT and the traditional transmissions. The experimental results show that the robustness is greatly enhanced by this adaptive scheme and the results show

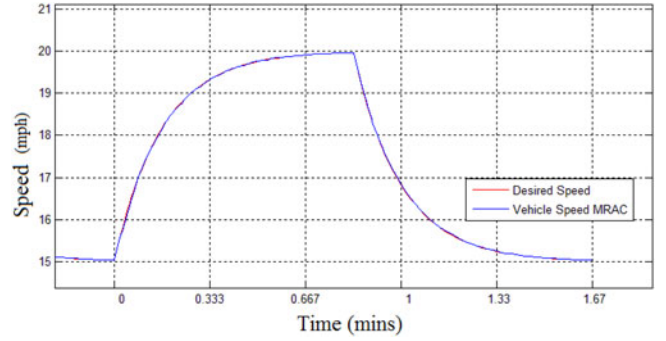


Fig. 8. Response of the comfortable car.

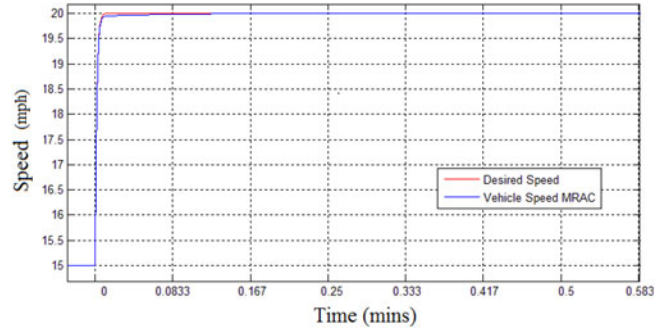


Fig. 9. Response of the sporty car.

excellent convergence to the desired speed under various conditions. In addition performance of the proposed controller is also evaluated for:

- 1) selection of desired driving mode,
- 2) sensitivity investigation of the response of the MRAC controller under the selection of various operating conditions with traditional transmission, and
- 3) experimental validation of the MRAC used in an HDCT bus and a simulation study to compare the results of the proposed MRAC with the conventional controller.

A. Driving Selection Modes

Our first experiment aims to

- 1) Comfortable Car:

This mode has smooth shifting with no sense of any gear change, therefore, it takes longer to reach the desired value, as shown in Fig. 8.

$$\text{Desired Model: } \frac{dv}{dt} = -0.1(v_d - v)$$

- 2) Sporty Shifting Car:

This mode allows the driver to feel the shifting of the transmission and have the manual transmission experience; it takes less time to reach the desired value, as shown in Fig. 9.

$$\text{Desired Model: } \frac{dv}{dt} = -10(v_d - v)$$

B. Sensitivity Analysis of the MRAC Controller

a) *Case 1: Speed is constant, Throttle is varying:* Increasing the engine throttle angle will cause the engine torque to increase, as shown between time 200 s thru 250 s in Fig. 10(a), for example. The vehicle acceleration changes and the engine torque responds proportionally to the throttle; the engine accelerates to produce more torque and the controller reduces the motor torque

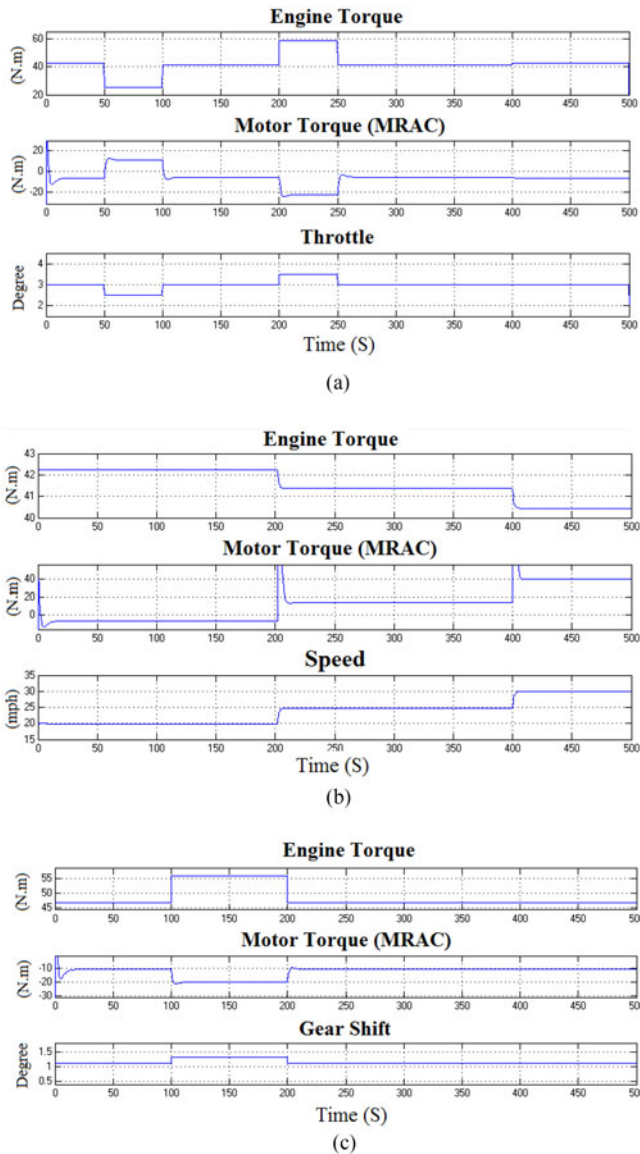


Fig. 10. Simulation results. (a) Varying throttle. (b) Varying speed. (c) Changing gears.

by the same amount to maintain a balance. Similarly, reducing the engine throttle angle will cause the engine torque to decrease, as shown at time 50 s in Fig. 10(a). Thus, the electric motor will turn on to assist, and the MRAC controller will supply more voltage to the motor to compensate for the torque lost.

b) Case 2: Throttle is constant, Speed is varying: At higher speeds, the gasoline engine provides the primary power for the hybrid system, and the electric motor assists when extra acceleration is needed, such as for passing, stopping, or starting. Meanwhile, to meet the HEV's fast torque response, the MRAC supplies more voltage and an additional acceleration is imposed on the motor torque [see Fig. 10(b)]. Both the engine and motor torque are changing simultaneously to accommodate the change of speed. However, when the speed is varying, the contributions of the engine and the motor are inversely proportional to each other.

c) Case 3: Changing Gears: Shifting into a higher gear will result in an increase of engine power and can effectively reduce

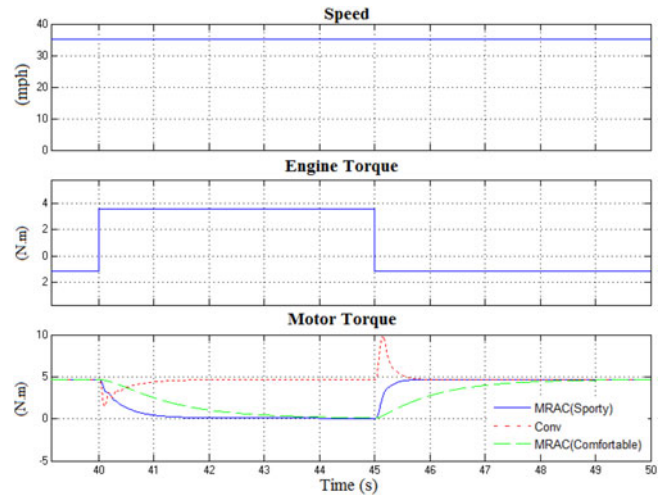


Fig. 11. Controllers' responses to speed changes. (a) MRAC's behavior. (b) MRAC versus conv.

the required motor torque. In contrast, when the transmission shifts to a low gear, as seen at time 200 s in Fig. 10(c), the MRAC will step up and supply more voltage to the motor to deliver higher torque in order to compensate for the power lost by the engine for smooth shifting and balancing.

C. The Hybrid Dual Clutch Transmission

The power loss during gear shifting is attributed only to clutch losses during its engagement. At this point, we will see power lost on the engine side. The MRAC-controlled motor will compensate for this power lost while changing gears or suddenly accelerating. During the driveline process, the speed will increase, so eventually more power is required by the HDCT design. The MRAC-controlled motor will produce more voltage to assist the engine in delivering the required torques to achieve the desired speed. As shown in Fig. 11(a), the MRAC and the engine torques assist each other at time 20 s to bring the vehicle speed up to the proper value; the comfortable mode, MRAC-comfortable, is producing the torque slower than the sporty mode, for the sake of its smoother shifting. On the other hand, the MRAC-sporty mode reaches the desired value faster and produces more voltage than required. Shifting gears with the DCT will result in losing some engine power and can affect the motor torque. So the motor will deliver extra power to compensate for the power lost, as seen at times 24 s and 28 s in Fig. 11(a). To look closely at the system when shifting gears, refer to the time from 28 s to 29 s in Fig. 12(a), when the DCT is shifting from second to third gear. The engine is losing some torque when the DCT clutch pressure of the second gear is decreasing. However, when the third gear is engaged, the engine is gaining extra power and moving forward to drive the powertrain system. During this operation of gear shifting, the sporty mode controller is producing extra torque as a result of the fast response by the motor to compensate for the power lost by the engine: in this situation, the driver will feel the mode transition and more acceleration will result in vehicle jerk. On the other hand, the comfortable mode controller compensates with the correct amount that was lost, using a longer time, for the sake of smooth shifting and balancing.

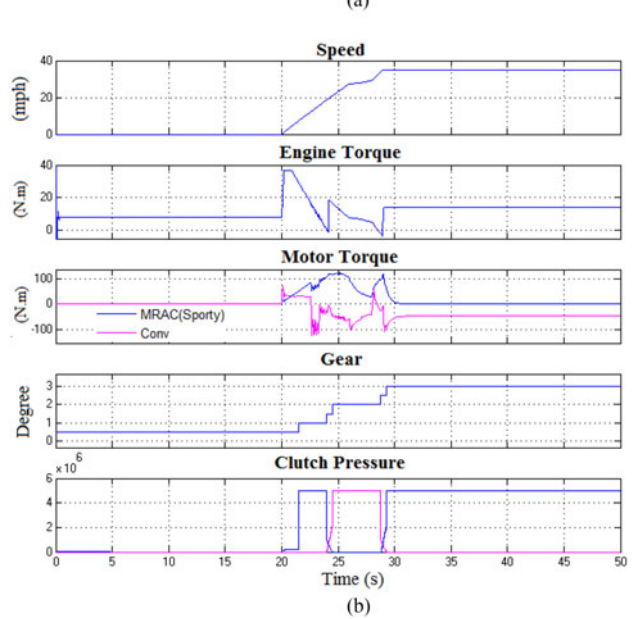
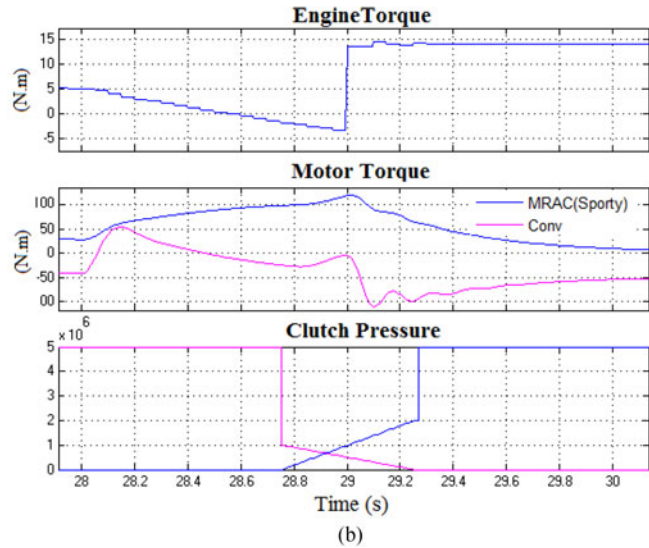
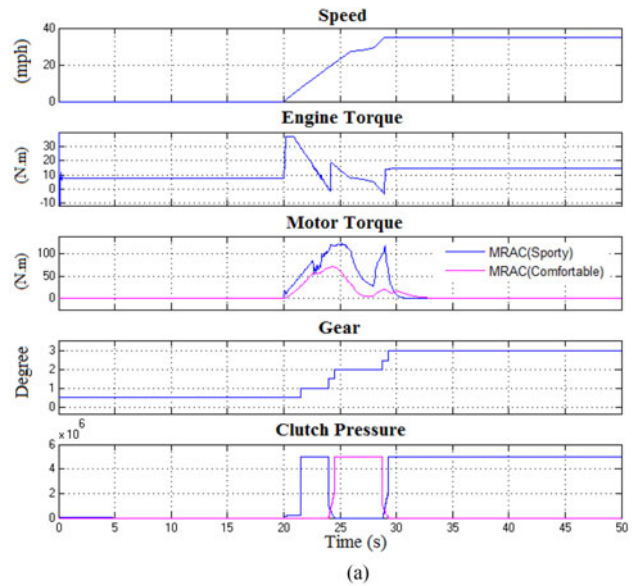
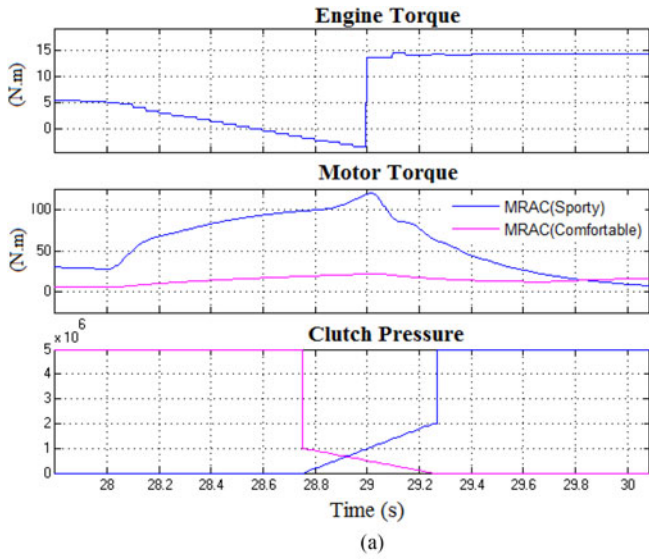


Fig. 12. DCT gear shift. (a) MRAC controllers. (b) MRAC versus conv.

Fig. 13. Engine throttle is varying with DCT. (a) MRAC’s Behavior. (b) MRAC Versus Conv.

D. Comparison With the Conventional Method

We consider the scenario of a typical drive-line process (the desired vehicle speed is changing) and compare the performance of the MRAC controller with the results of conventional operation (abbreviated by Conv.). The MRAC motor has boosted more torque to compensate for torque deficits by the engine when the gear is changing to maintain balance, whereas that of Conv. falls by 100 points at the end of the third gear at time 29 s, as shown in Fig. 11(b). For Conv., the profile of the vehicle speed is similar, which implies that the clutch torque negatively affects the vehicle acceleration and causes the engine torque to decline. Moreover, the motor torque in the MRAC does not compensate for this negative effect, as shown in Fig. 12(b). Thus, the vehicle speed has to fall. However, the MRAC avoids this situation by increasing the traction motor torque to compensate for the negative effect. No substantial vehicle jerk occurs in the MRAC control simulation, even with a sudden change of the engine throttle. The MRAC scheme prevents the motor response from a large overshoot: in the comfortable mode it slowly com-

pensates for the lost torque, and does this more quickly in the sporty mode. However, a sudden vehicle jerk of over 10 points is found in the results from the conventional controller at time 45 s, as shown in Fig. 13. The reason for the sudden jerk is that Conv. cannot react quickly enough to the changes: the Conv.-controlled motor is clearly slower than the MRAC-controlled system. Finally, the performance of the Conv. controller quickly deteriorates, whereas the performance of the MRAC controller remains good. Obviously, the MRAC controller can considerably improve the behavior of the motor in terms of this criterion.

It can be concluded that the HDCT design is more efficient than the conventional design in all conditions. Although the HDCT design improves the efficiency of the motor in compensating for all power lost in the system, it deteriorates the overall efficiency of the powertrain itself.

VII. CONCLUSION

A model reference adaptive control (MRAC) has been designed for the stability of a closed loop system in the sense of Lyapunov. The MRAC takes the driving vehicle as the reference model, and the controller acts on the output errors between the reference model and the vehicle as the feedback signals to achieve smooth and efficient performance. The proposed MRAC is applied to a hybrid electric vehicle with dual clutch transmission (HDCT), and has yielded good performance under different conditions, which implies that the MRAC is adaptive to different torque distribution strategies. The current study, which was performed on the adaptive control applications, reveals that the Lyapunov method is working properly. The simulation results confirm that the MRAC outperforms the conventional operation method for an HDCT by reducing the vehicle jerk and the torque interruption for the driveline. Therefore, this paper shows that MRAC is very promising. Further studies are underway to treat vehicles with dual clutch transmission during mode transitions.

REFERENCES

- [1] P. Waltermann, "Modeling and control of the longitudinal and lateral dynamics of a series hybrid vehicle," in *Proc. IEEE Int. Conf. Control Appl.*, 1996, pp. 191–198.
- [2] B. Conlon, "Comparative analysis of single and combined hybrid electrically variable transmission operating modes," *SAE Tech. Paper* 2005–01-1162, 2005.
- [3] M. P. R. V. Rao and A. Hassan, "New adaptive laws for model reference adaptive control using a non-quadratic Lyapunov function," in *Proc. 12th IEEE Mediterranean Electromech. Conf.*, Dubrovnik, Croatia, May 12–15, 2004, pp. 371–374.
- [4] L. Yacoubi, K. Ai-Haddad, L.-A. Dessaint, and F. Fnaiech, "Linear and nonlinear control techniques for a three-phase three-level NPC boost rectifier," *IEEE Trans. Ind. Electron.*, vol. 53, no. 6, pp. 1908–1918, Dec. 2006.
- [5] K. Upendra, "Dual clutch transmission for plug-in hybrid electric vehicle comparative analysis with Toyota hybrid system," Master's Thesis, Chalmers University Technology, Göteborg, Sweden, 2014.
- [6] P. Ioannou and B. Fidan, *Adaptive Control Tutorial* (Advances in Design and Control), vol. 11. Philadelphia, PA, USA: Society for Industrial and Applied Mathematics, 2006.
- [7] M. P. R. V. Rao, "Non-quadratic Lyapunov function and adaptive laws for MRAC," *IEE Electron. Lett.*, vol. 23, no. 23, pp. 2278–2280, Nov. 1998.
- [8] S. Coman and C. Boldisor, "Model reference adaptive control for a DC electric drive," *Bulletin Transilvania Univ. Braov, Ser. I: Eng. Sci.*, vol. 6, no. 2, 2013.
- [9] I. Landau *et al.*, *Adaptive Control: Algorithms, Analysis and Applications*. London, U.K.: Springer-Verlag, 2011.
- [10] K. S. Narendra and L. S. Valavani, "Stable adaptive controller design direct control," *IEEE Trans. Automat. Control*, vol. 23, no. 4, pp. 570–583, Aug. 1978.
- [11] K. K. Shyu, M. J. Yang, Y. M. Chen, and Y.-F. Lin, "Model reference adaptive control design for a shunt active-power-filter system," *IEEE Trans. Ind. Electron.*, vol. 55, no. 1, pp. 97–106, Jan. 2008.
- [12] C. B. Kadu, B. J. Parvat, and N. N. Parekar, "Modified MRAC for controlling water level of boiler system," in *Proc. Int. Conf. Comput. Intell. Commun. Netw.*, 2015, pp. 1537–1539.
- [13] Y. T. Liu, K. M. Chang, and W. Z. Li, "Model reference adaptive control for a piezo-positioning system," *Precision Eng.*, vol. 34, no. 1, pp. 62–69, 2010.
- [14] Z. Zhao, H. Chen, and Q. Wang, "Control and real-time optimization of dry dual clutch transmission during the vehicle's launch" Hindawi Publishing Corporation, Cairo, Egypt, vol. 2014, Art. no. 494731.
- [15] L. Chen, G. Xi, and J. Sun, "Torque coordination control during mode transition for a series-parallel hybrid electric vehicle," *IEEE Trans. Veh. Technol.*, vol. 61, no. 7, pp. 2936–2949, Sep. 2012.
- [16] J. Zhang, L. Chen, and G. Xi, "System dynamic modelling and adaptive optimal control for automatic clutch engagement of vehicles," *Proc. Inst. Mech. Eng., Part D, J. Automobile Eng.*, vol. 216, no. 12, pp. 983–991, Dec. 2002.
- [17] A. Crowther, N. Zhang, D. K. Liu, and J. K. Jeyakumaran, "Analysis and simulation of clutch engagement judder and stick-slip in automotive powertrain systems," *Proc. Inst. Mech. Eng., Part D, J. Automobile Eng.*, vol. 218, no. 12, pp. 1427–1446, Dec. 2004.



Walid Elzaghbir received the B.S. degree and the M.S. degrees from the University of Michigan-Dearborn, Dearborn, MI, USA, in 2004 and 2009, respectively, all in electrical engineering. He is currently working toward the Ph.D. degree in the Department of Electrical Engineering. He joined the ITT as an Electronic Teacher in 2009.



Yi Zhang received the B.S. degree from Central South University, Changsha, China, in 1982, and the M.S. and Ph.D. degrees from the University of Illinois at Chicago, Chicago, IL, USA, in 1986 and 1989, respectively, all in mechanical engineering. He joined the University of Michigan-Dearborn, Dearborn, MI, USA, in 1992 and is currently an Associate Professor of mechanical engineering. His teaching and research interests include the areas of gear design and manufacturing, theory of gearing, mechanical design, and vehicle powertrains. He has published

more than 40 technical papers in gear design and power transmission areas. He is a member of ASME.



Narasimhamurthi Natarajan received the Graduate degree from Ramakrishna Mission High School Vivekananda Junior College and the Indian Institute of Technology Madras, Chennai, India before coming to the US in 1974 and the Master's and Ph.D. degrees from the University of California Berkeley, Berkeley, CA, USA. He received the Ph.D. degree at the age of 26 and after a year as faculty at Washington University in St. Louis. He is an Associate professor in the Department of Electrical Engineering, University of Michigan-Dearborn, Dearborn, MI, USA.



Frank Massey received the Bachelor's degree in mathematics from the University of California at Los Angeles, Los Angeles, CA, USA, and the Ph.D. degree in mathematics from the University of California at Berkeley, Berkeley, CA, USA.

He joined the University of Michigan-Dearborn in 1978 after teaching for seven years at the University of Kentucky.

His teaching and research interests include applied mathematics with particular interest in probability and differential equations.



Chunting Chris Mi (S'00–A'01–M'01–SM'03–F'12) received the B.S.E.E. and M.S.E.E. degrees in electrical engineering from Northwestern Polytechnical University, Xian, China, and the Ph.D. degree in electrical engineering from the University of Toronto, Toronto, ON, Canada. He was a Professor of electrical and computer engineering and the Director of the Department of Energy-funded Graduate Automotive Technology Education Center for Electric Drive Transportation, University of Michigan, Dearborn, MI, USA. He joined San Diego State University as a

Professor and Chair in the Department of Electrical and Computer Engineering in Fall 2015.